Science of the Total Environment 643 (2018) 1248–1256

Contents lists available at ScienceDirect

Science of the Total Environment

journal homepage: www.elsevier.com/locate/scitotenv

Dasymetric mapping of urban population in China based on radiance corrected DMSP-OLS nighttime light and land cover data

Xiaoma Li [a,b], Weiqi Zhou [b,c,*]

[a] Horticulture and Landscape College, Hunan Agricultural University, Changsha 410128, PR China
[b] State Key Laboratory of Urban and Regional Ecology, Research Center for Eco-Environmental Sciences, Chinese Academy of Sciences, Beijing 100085, PR China
[c] University of Chinese Academy of Sciences, Beijing 100049, PR China

HIGHLIGHTS

- Urban nighttime light (UNTL) is produced using NTL and urban land data.
- We disaggregated county level urban population (UP) using 1 km UNTL in China.
- We created 1 km resolution UP datasets in China in 2000 and 2010.
- UP increased in suburban areas of the big cities during 2000 and 2010.
- UP decreased in urban center of big cities and small towns during 2000 and 2010.

GRAPHICAL ABSTRACT

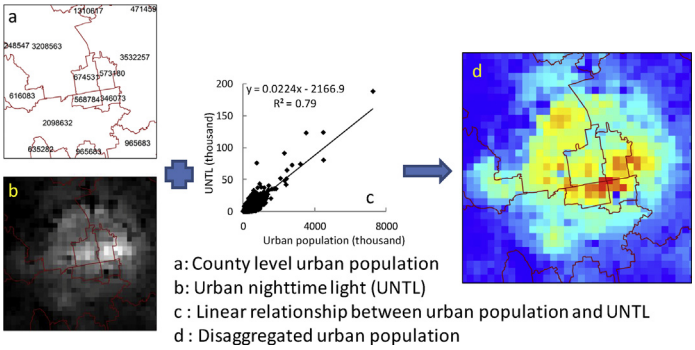

a: County level urban population
b: Urban nighttime light (UNTL)
c : Linear relationship between urban population and UNTL
d : Disaggregated urban population

ARTICLE INFO

Article history:
Received 16 January 2018
Received in revised form 15 May 2018
Accepted 19 June 2018
Available online 4 July 2018

Editor: SCOTT SHERIDAN

Keywords:
Disaggregate
Population distribution
Population density
Urbanization
Nighttime light
Urban population

ABSTRACT

High spatial resolution urban population dataset is increasingly required for sustainable urban planning and management. Dasymetric mapping is an effective approach to create such dataset. However, the created gridded total population datasets usually have limitation for urban analysis in developing countries as they usually underestimate urban population because of the strong urban-rural difference. In this study, we aimed to create a dataset of gridded urban population with 1 km resolution in China in year 2000 and 2010. We proposed an index of urban nighttime light (UNTL) by integrating radiance corrected DMSP nighttime light (RcNTL) and urban land, which is then used as weight to disaggregate county-level urban population. The validation using township population in Beijing as references shows reasonable accuracy with a mean relative error of 38% and a R^2 of 68%. Using only two widely available datasets (RcNTL and urban land), the proposed method is simple and computing efficient compared with methods using multiple geospatial data (e.g., land use and land cover, distance to city center, slope) and that combined with remote sensing imagery. As the used two auxiliary datasets are accessible globally, the method has great potential to produce similar urban population dataset for other developing countries where fine scale census population datasets are scarce. The produced urban population dataset is valuable for enriching our understanding of the urbanization process and designing sustainable urban planning and management strategies in China.

© 2018 Elsevier B.V. All rights reserved.

1. Introduction

Accounting for more than half of global population, urban areas are hot spots of global sustainability as they are the center of socioeconomic

* Corresponding author.
E-mail address: wzhou@rcees.ac.cn (W. Zhou).

https://doi.org/10.1016/j.scitotenv.2018.06.244
0048-9697/© 2018 Elsevier B.V. All rights reserved.

development, natural resource consumption, and waste emission (Acuto et al., 2018; Grimm et al., 2008; Seto et al., 2014). Population is the fundamental agent in the urban ecosystem. Its spatial distribution has strong heterogeneity and significantly impact the structure and process of urban ecosystem (Creutzig et al., 2015; Güneralp et al., 2017). A better understanding of urban population distribution has a fundamental role for urban planning and management, urban growth simulation, urban environment modeling, and public health assessment, among others (Langford et al., 2008; Maantay and Maroko, 2009; Mennis, 2015).

Census population reported as the aggregated number of spatial/administrative units is the most widely available dataset (Huang et al., 2016; NBSC, 2012; United Nations, 2014). However, it cannot satisfy the demand for urban study because 1) it cannot reflect the spatial heterogeneity of population within the spatial unit, which can be significant especially when the spatial unit has a large spatial extent and population distribution potentially has large variations in space. This is particularly true in developing countries; 2) it is not computable with other environmental data (e.g., gridded temperature and air pollutant) for environmental analysis; and 3) it is not temporally compatible because of the frequent change of the spatial unit boundary, even though some solutions have been developed (Holt et al., 2004; Ruther et al., 2015; Schroeder, 2007; Zoraghein et al., 2016). Disaggregating census population to create gridded population dataset at finer resolution is an effective approach to solve these problems (Balk et al., 2006; Dobson et al., 2000; Mennis, 2015; Stevens et al., 2015; Su et al., 2010; Sun et al., 2017; Wu et al., 2005).

Several types of dasymetric mapping methods have been developed (reviewed in the next section) and a number of gridded population (or population density) datasets have been created for single city (e.g., in Philadelphia, U.S. (Mennis, 2015), in Cardiff, South Wales (Langford et al., 2008), in Barcelona, Spain (Pavía and Cantarino, 2017)), nationally (e.g., in China (Gaughan et al., 2016; Tan et al., 2018; Wang et al., 2018), in U.S. (Dmowska and Stepinski, 2017)), regionally (e.g., in Europe (Gallego, 2010; Silva et al., 2013), in Africa, Asia and Latin America (Stevens et al., 2014), and globally (e.g., LandScan (Bright et al., 2011) and Gridded Population of the World (GPW) (CIESIN, 2017)). Despite the success in capturing spatial details of population, the disaggregated population datasets usually overestimate population in low-density areas and underestimate population in high-density areas (e.g., urban areas), mainly because urban and rural areas have different characteristics in urban infrastructures (including magnitude and spatial pattern) and intensity of human activities, and the developed proxy variable failed in capturing this urban-rural difference (Cockx and Canters, 2015; Gaughan et al., 2016; Harvey, 2002; Mao et al., 2012; Mennis, 2010; Mennis and Hultgren, 2006). For example, buildings in the urban areas are usually higher than that in the rural areas, so is population density. If the auxiliary datasets do not reflect this variation well, urban population will be allocated to rural areas and the disaggregated population dataset will underestimate urban population. This underestimation is more severe when the census unit has a large spatial extent and contains areas along the urban-rural continuum.

Even though potentially underestimated, the disaggregated total population with very high spatial resolution (<100 m) in developed countries can capture spatial variation of urban population well (Astrudmaantay et al., 2007; Bajat et al., 2013; Holt et al., 2004; Joseph et al., 2012; Langford et al., 2008; Mennis, 2010, 2015; Pavía and Cantarino, 2017; Salvatore et al., 2005; Tomás et al., 2016). However the underestimation of urban population by disaggregating total population in developing countries (e.g., China) is much more severe because of 1) stronger urban-rural difference in population density and urban infrastructure, 2) a larger spatial extent of the census unit which includes both urban and rural areas, and 3) higher proportion of rural population. Two potential approaches could be adopted to address this issue. One is to integrate auxiliary data which better captures the variation of population distribution between urban and rural areas. For example, the 3 dimension (3D) variables (e.g., floor area, building volume) usually achieve higher accuracy than the 2 dimension (2D) variables (e.g., building footprint, impervious surface area) (Filip et al., 2016; Pavía and Cantarino, 2017). The other is to disaggregate urban and rural population separately (Azar et al., 2010; Sun et al., 2017; Zhuo et al., 2009).

China has experienced rapid urbanization since 1978 with urbanization level increasing from 17.9% to 58.5% in 2017. It is projected that another 0.3–0.4 billion people will reside in the urban areas till 2050. Understanding the spatial distribution of urban population and its temporal change is highly required for sustainable urban planning and management. A number of gridded datasets of total population in China have been developed by disaggregating county-level population based on a series of geospatial datasets and remote sensing imagery (Gaughan et al., 2016; Tan et al., 2018; Wang et al., 2018; Yu et al., 2018; Zeng et al., 2011; Zhuo et al., 2009). However, these datasets may underestimate urban population for the reason discussed above and thus increase uncertainty in subsequent analysis (Cockx and Canters, 2015; Gaughan et al., 2016).

Based on rich experience in dasymetric population mapping using geospatial data and remote sensing data as auxiliary dataset, this study aims to: 1) create a 1 km resolution gridded urban population dataset of 2000 and 2010 in China by disaggregating county-level urban population using nighttime light (NTL) and land cover data as auxiliary datasets, and (2) understand the spatiotemporal pattern of urban population in China during 2000 and 2010. The developed urban population dataset can better capture the spatiotemporal pattern of urban population than currently available datasets (e.g., gridded total population), and is valuable for sustainable urban planning and management in China.

2. Methods of dasymetric population mapping

Dasymetric mapping, also called dasymetric modeling is a kind of areal interpolation, which aims to disaggregate coarse resolution variable (e.g., population) to finer resolution based on auxiliary data (Bajat et al., 2013; Eicher and Brewer, 2001; Mennis, 2009; Mennis, 2010; Nagle et al., 2014; Pavía and Cantarino, 2017; Wright, 1936). Dasymetric population mapping has a long history but gets popular thanks to the rapid development of geographic information system and satellite remote sensing. Its key idea is to produce a weight layer (mostly gridded), based on which census population is disaggregated assuming the same spatial distribution of population and the weight layer within the spatial unit (Dmowska and Stepinski, 2017; Gallego et al., 2011; Mennis, 2009; Mennis, 2015; Nagle et al., 2014; Stevens et al., 2015; Su et al., 2010; Wu et al., 2005). The general formula is expressed as:

$$P_i = \frac{P}{\sum_{i=1}^{n} W_i} \times W_i \quad (1)$$

where P_i is population of the ith grid cell, W_i is the weight of the corresponding grid cell, n is the number of grid cells within the spatial unit, and P is total population of the spatial unit. Therefore, the critical step is to prepare the weight layer, namely to calculate W_i.

The definition, history, principles, and methods of dasymetric population mapping have been overviewed in other papers (Astrudmaantay et al., 2007; Eicher and Brewer, 2001; Mennis, 2009; Mennis, 2015; Wu et al., 2005; Zoraghein et al., 2016). Here we mainly focused on how the weight layer is produced and generally classified them into two groups: classified weight and continuous weight.

2.1. Dasymetric population mapping based on the classified weight

Classified weight means the weight layer is composited by several classes with each has the same value. Area weighting, the simplest

dasymetric mapping method, belongs to this group as the weight layer has only one class. In other words, area weighting assigns an equal weight (e.g., population density) for all grids within the spatial unit assuming the population is evenly distributed. However, this assumption is usually not satisfied in reality and produces large errors (Astrudmaantay et al., 2007; Mennis, 2009; Mennis and Hultgren, 2006; Su et al., 2010). To increase the accuracy, classified auxiliary data (e.g., inhabited land, land use and land cover (LULC)) are integrated. The so-called binary area weighting with the weight layer coded as either 0 or 1, employs a binary map (inhabited and uninhabited) to evenly disaggregate population to inhabited land (Langford, 2007; Mennis, 2015; Su et al., 2010). The weight layer with multiple classes is developed with the aid of auxiliary data (e.g., LULC) to increase the accuracy, and is widely applied, such as in the European Union (Gallego, 2010), in East Africa (Tatem et al., 2007), in Southeast Asia (Gaughan et al., 2013), in U.S. (Dmowska and Stepinski, 2017), and in China (Mao et al., 2012). Increasing the classes of the weight layer can increase the accuracy (Dmowska and Stepinski, 2017; Qi et al., 2015; Su et al., 2010), but it still cannot capture the population variation within each class.

2.2. Dasymetric population mapping based on the continuous weight

To solve the limitation of classified weight, continuous weight is developed thanks to the increasing availability of auxiliary data and the increase of computing power. The continuous weight can also be recognized as one type of special classified weight with numerous classes. Impervious surface area, a measure of percent developed land can generate higher accuracy than classified LULC data (Azar et al., 2010; Li and Lu, 2016; Silva et al., 2013). However, impervious surface area only captures the horizontal development intensity, but has no information of the vertical development intensity. Building volume considering both footprint and height of buildings is demonstrated to be a more accurate index to disaggregate census population (Bajat et al., 2013; Biljecki et al., 2016; Calka et al., 2016; Filip et al., 2016; Kressler and Steinnocher, 2008; Pavía and Cantarino, 2017; Tomás et al., 2016; Ural et al., 2011). However, this method is only tested in small areas mostly in developed countries, and not widely applicable in developing countries as the data of building volume is usually not available and extracting this information from high spatial resolution remote sensing imagery or light detection and raging (LiDAR) data is time and labor consuming. Recently, the increasingly available geospatial big data (e.g., point of interesting data, road network, etc.) are demonstrated a useful weight to disaggregate urban population (Bakillah et al., 2014; Langford et al., 2008; Lin and Cromley, 2015; Reibel and Bufalino, 2005; Yao et al., 2017; Zandbergen, 2011).

Most applications, especially for large areas, generate the continuous weight using auxiliary geospatial data and remote sensing data, by developing the statistical relationship between population and a series of explanatory variables. The commonly used geospatial variables include: distance based variable (e.g., distance to urban, river, road, etc.), topographic variable (e.g., elevation, slope, etc.), and LULC data, among others (Azar et al., 2013; Bajat et al., 2011; Bryan and Brian, 2013; Dong et al., 2015; Lung et al., 2013; Mao et al., 2012; McKee et al., 2015; Wang and Zhou, 1999; Yue et al., 2005). NTL, specifically that from Defense Meteorological Satellite Program (DMSP) measures light emission from human activities and can be used to disaggregate population, especially for large areas (Elvidge et al., 1999; Sutton, 1997; Sutton et al., 1997). However, DMSP NTL has the problem of saturation and overglow effect (Wang et al., 2018; Yang et al., 2013). In practice, NTL and geospatial data are combined together to produce the continuous weight layer through statistical analysis (Briggs et al., 2007; Gaughan et al., 2016; Stevens et al., 2014; Tan et al., 2018; Wang et al., 2018; Zeng et al., 2011).

3. Datasets

County-level urban population in China in 2000 and 2010 were obtained from the database of the fifth and sixth census, respectively (NBSC, 2002, 2012). Our study area is the mainland of China and does not include Hong Kong, Macao, and Taiwan. County is the fourth administrative level in the order of nation, province, prefectural city, county/district, and subdistrict/town/country. County is the finest level, at which urban population is reported in China. In this dataset urban population is defined as population residing in city and town proper, and their surrounding areas developed with municipal utilities and public facilities (NBSC, 2012).

NTL data in 2000 and 2010 used in this study were the radiance corrected DMSP NTL (RcNTL) downloaded from National Geophysical Data Center (NGDC). DMSP NTL has been widely used to disaggregate population (Bhaduri et al., 2007; Briggs et al., 2007; Song et al., 2015; Sutton, 1997; Yang et al., 2013; Zeng et al., 2011; Zhuo et al., 2009). It is collected at high gain settings and suffers from saturation that digital numbers of bright areas (e.g., urban center) are set as 63 even though they are much brighter. Several indices are put forward to mitigate the saturation problem by incorporating optical remote sensing images, but they still produce some uncertainty (Sun et al., 2017; Wang et al., 2018; Yang et al., 2013). NGDC corrected the saturation of DMSP NTL by merging images collected at three fixed-gain levels (low, medium and high) and released eight global datasets of RcNTL from 1996 to 2010 (Hsu et al., 2015). RcNTL is reported linearly correlated with socioeconomic variables such as population, GDP, electric power consumption, etc. (Cao et al., 2016; Elvidge et al., 1999). We used RcNTL to disaggregate urban population in China in this study.

ChinaCover (2000 & 2010), land cover datasets were used to determine the location of urban population (i.e., urban land). These datasets were used as urban masks to solve the overglow problem of RcNTL and avoid urban population being allocated to nonurban land which is next to urban land with high NTL value (Silva et al., 2013; Sun et al., 2017). ChinaCover 2010 was produced from 30 m Landsat imagery and HJ-1 imagery using knowledge-based visual interpretation and object-oriented automatic classification technology, and ChinaCover 2000 was produced using the change detection method based on ChinaCover 2010 and Landsat imagery in 2000 (Wu et al., 2014). ChinaCover includes six major classes: forest and shrub, grassland, wetland, croplands, artificial land (i.e., developed land), and bare land. The overall accuracy of the classification is 94% (Wu et al., 2014). The artificial land includes all developed impervious surface area for both urban and rural settlements. ChinaCover was developed by the Chinese Academy of Sciences and has been used for assessing national ecosystem changes between 2000 and 2010 (Ouyang et al., 2016; Xu et al., 2017).

4. Methods

We developed a continuous weight layer, urban RcNTL (UNTL), which measures RcNTL on urban land, to disaggregate county-level urban population in China. The rationale of this index as a proxy to disaggregate urban population lies in: 1) RcNTL effectively solves the

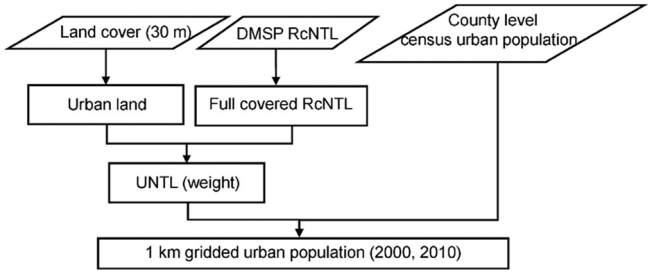

Fig. 1. Flowchart of disaggregating urban population using RcNTL and land cover data.

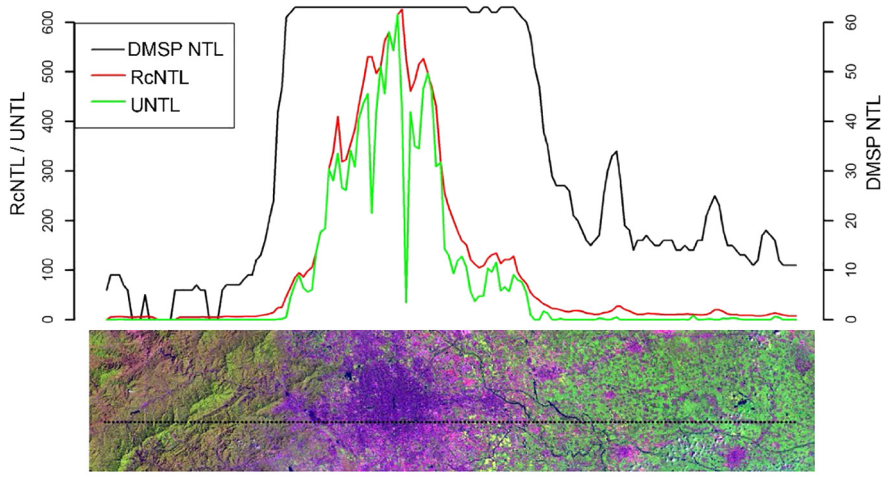

Fig. 2. DMSP NTL, RcNTL, and UNTL along an urban-rural transect in Beijing in 2010.

saturation problem of DMSP NTL and captures the local variation of human activity and population distribution; and 2) the urban land is used as a mask layer to solve the overglow problem of RcNTL and avoids urban population being allocated to undeveloped land, for example, those close to urban land with high NTL values. In each county, we used Eq. (1) to estimate urban population for each grid cell using the UNTL as the weight. In other words, we first estimated the number of persons per unit of UNTL for each county and then multiplied it with the UNTL for each grid cell within the county to obtain urban population for the corresponding grid cell. Since the parameter (i.e., person per unit of UNTL) varies county by county, this dasymetric mapping approach accounted for the spatial non-stationary relationship between urban population and UNTL well (Cockx and Canters, 2015; Dmowska and Stepinski, 2017; Mennis, 2009; Wang et al., 2018). Fig. 1 shows the flowchart of the procedure.

We delineated urban land based on the class of artificial land from ChinaCover (Wu et al., 2014). The class of artificial land maps all types of developed impervious land, including continuous urban built-up areas, towns, and rural settlements. Based on the national bureau of statistics of China (NBSC), urban population are population residing in city and town proper, and their surrounding areas developed with municipal utilities and public facilities (NBSC, 2012). Therefore, we used a threshold of patch size to map the urban land from the artificial land as that did by Deng et al. (2015) and Yue et al. (2013), because patches of rural settlements are smaller than that of urban patches. Considering the regional variation of patch size of the rural settlement in China, for example larger settlement in plain areas and smaller settlement in mountainous areas, thresholds of 0.5 km^2 and 0.1 km^2 were applied, respectively for plain areas and mountainous areas (Deng et al., 2015; Yue et al., 2013).

We found that urban population not only reside in big cities with high RcNTL values (e.g., Beijing), but also live in small towns even without RcNTL values, for example in remote and less developed areas with much lower population density and less economic activity. This phenomenon is also reported in other studies (e.g., Wang et al. (2018)). This means the unlit areas in the RcNTL data such as small towns also have urban population. The omission of these small cities/towns may generate large uncertainty as their population will be allocated to the lit areas. To address this problem, we produced a full covered RcNTL by setting the RcNTL value of the unlit area as the minimum value of the corresponding county.

We overlaid RcNTL and urban land to generate UNTL. As these two datasets have different spatial resolutions, we aggregated urban land to 1 km resolution by calculating percent urban land for each RcNTL pixel and multiplied it with RcNTL as the continuous weight. Another choice is to resample RcNTL to match the resolution of urban land. We did not adopt this approach because it could only slightly improve the accuracy (Fig. S2 in supplementary data) but dramatically increased computing time for the national application of China. Finally we disaggregated county-level urban population to create a 1 km resolution dataset for 2000 and 2010.

We tested the accuracy of the disaggregated urban population using township (subdistrict) population in Beijing in 2010 (NBSC, 2012) as an example because such dataset in other areas was not available. The detail of the validation data is described in the Supplementary data. We calculated the mean relative error (MRE) to test the accuracy (Pavía and Cantarino, 2017; Su et al., 2010; Sun et al., 2017; Yang et al., 2013).

$$RE = \frac{Pd_i - Po_i}{Po_i} \times 100\% \quad (2)$$

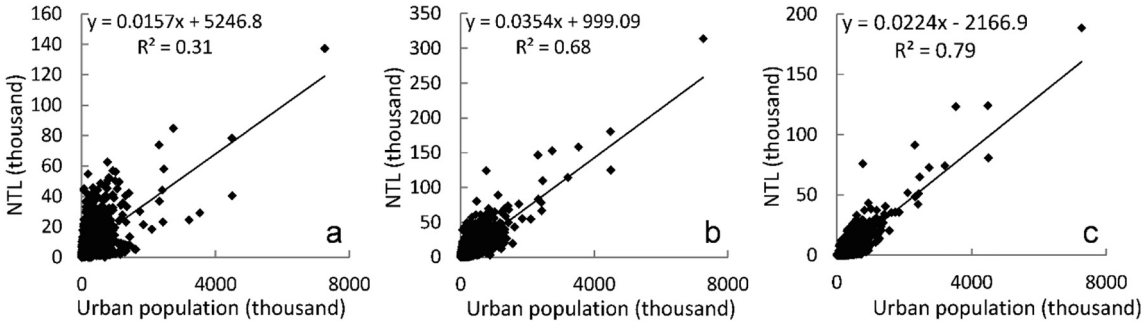

Fig. 3. Relationship between urban population and NTL (a: DMSP NTL, b: RcNTL, c: UNTL) in 2010 at county level in China.

$$\mathrm{MRE} = \frac{\sum_{i=1}^{n} |\mathrm{RE}_i|}{n} \quad (3)$$

where RE_i is relative error of the ith town, Pd_i and Po_i are the disaggregated and observed/reported population for the corresponding subdistrict, respectively. MRE is mean relative error.

5. Results and discussion

5.1. The ability of UNTL to disaggregate urban population

Fig. 2 shows the variations of DMSP NTL, RcNTL, and UNTL along an urban-rural transect in Beijing in 2010. It clearly shows that DMSP NTL had no variation in the urban center because of its saturation problem. The RcNTL solved the saturation problem well, displaying much larger range and stronger spatial variation. However, RcNTL still suffered from the problem of overglow as the uninhabited land near urban also had high values. For example, the pixel of Temple of Heaven Park, located in southeast corner of the old city displayed very high RcNTL. However, the observed light was not emitted by human activity of the pixel itself but from its neighboring pixels. In addition, the agricultural land in suburb and rural areas also had light signal even though there was no population. By integrating urban land data, the UNTL solved the problem of overglow and only mapped RcNTL on the urban land.

NTL shows linear correlation with urban population (Fig. 3). The DMSP NTL only explained 31% of the variance of county-level urban population, mostly because of its saturation problem. After correcting this, RcNTL improved the correlation and could explain about 70% of the variance in urban population. After excluding RcNTL belonging to nonurban land, the proposed index, UNTL shows much stronger correlation with urban population, explaining about 80% of the variance (Fig. 3c).

The validation analysis using census population of subdistrict (lower level than county) as reference in Beijing shows that the disaggregated urban population is highly correlated with the observed/reported urban population with R^2 of 0.68, and a mean relative error of 38% (Fig. 4). This accuracy is comparable or slightly higher than other studies for large areas (Dmowska and Stepinski, 2017; Sun et al., 2017), demonstrating the effectiveness of using UNTL to disaggregate county-level urban population in China. There is a similar mean relative error for the highly developed and less developed districts (37% and 39%, respectively), but R^2 was larger in less developed districts (85%) than that in highly developed districts (64%) (Fig. 4b, c). Population in a grid cell can be conceptualized as three dimensional volume determined by horizontal area and vertical height (density) (Alahmadi et al., 2013; Lu et al., 2011; Tomás et al., 2016). Therefore, disaggregating population is to solve a three dimensional problem, which can be decomposed as which land has urban population and how many persons are there. The UNTL successfully disaggregates urban population by using percent urban land to directly address the first question, and RcNTL to directly address the second question.

We also compared our disaggregated urban population with two other gridded population datasets (WorldPop and GPW) for those subdistricts used for validation assessment in Beijing (Fig. S1 in the Supplementary data). WorldPop in China is disaggregated from county-level total population based on a series of geospatial and remote sensing data (Gaughan et al., 2016; Stevens et al., 2015). Population disaggregated in our study had slightly lower mean relative error (38%) than WorldPop (40%) and GPW (42%), and higher R^2 (68%) than worldPop and GWP (59% and 56%, respectively) (Fig. 4a). The three gridded datasets showed similar accuracies for the highly developed districts (Fig. 4b), but our dataset showed higher accuracy for the less developed districts (Fig. 4c). WorldPop underestimated urban population in less developed districts by 43%, indicating urban population was allocated to non-urban land. The major reason could be that WorldPop did not explicitly distinguish urban population and rural population, and the corresponding urban land and rural settlements. Therefore, urban population were wrongly distributed to rural settlements. This is not a problem in our study because we only focused on urban population and urban land. In addition, we used the radiance corrected DMSP NTL which can better capture the spatial variation of human activity and

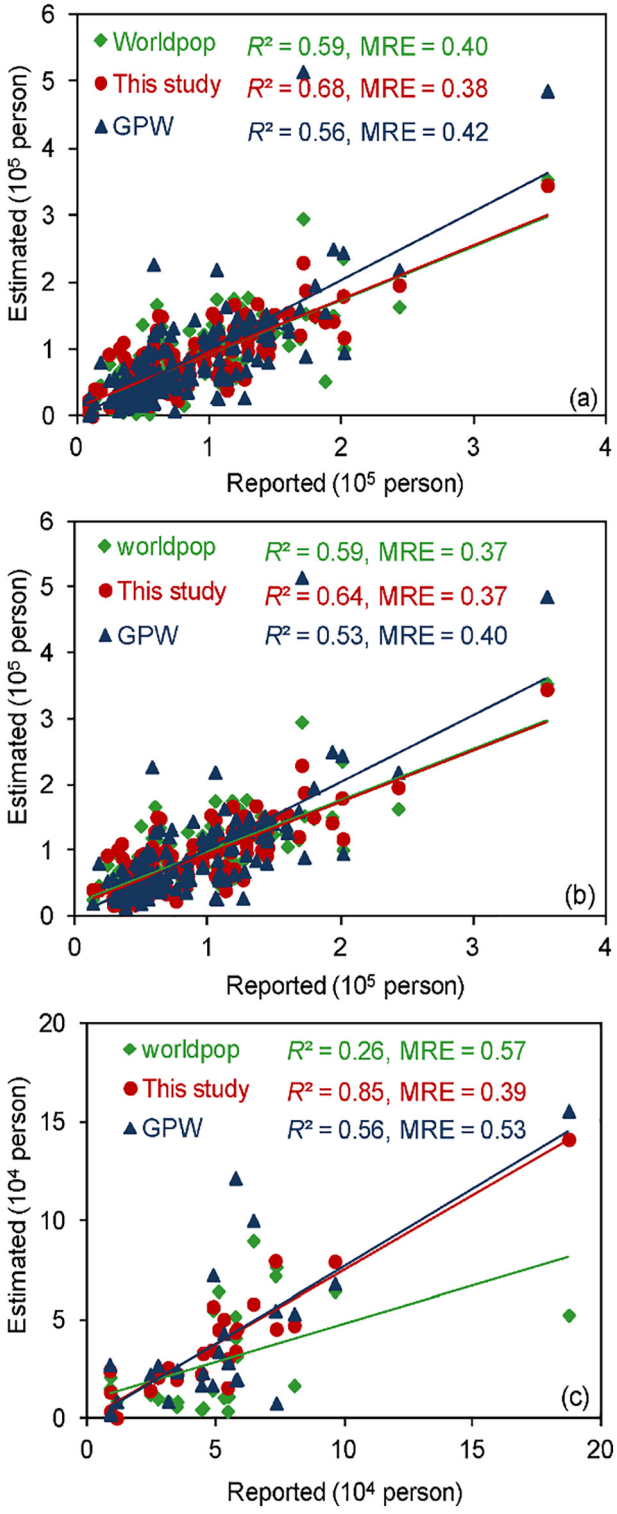

Fig. 4. Accuracy of the disaggregated urban population checked with subdistrict population in Beijing in 2010, and its comparison with another two datasets (WorldPop and GPW). (a: subdistricts in all districts, b: subdistricts in highly developed districts, c: subdistricts in less developed districts, see the location of these districts in Fig. S1 in the supplementary data).

population than the saturated DMSP NTL (Fig. 2). It should be noted that even though our data had higher accuracy, it still underestimated urban population in subdistricts of less developed districts by 24%. This may be because the urban land outside the subdistricts was over mapped.

With the increasing accessibility of geospatial data, complex model integrating multiple geospatial data and remote sensing image is usually used to disaggregate population (Azar et al., 2013; Stevens et al., 2015). However, our study demonstrated that the two datasets (RcNTL and urban land) can generate equal or higher accuracy than multiple geospatial data and remote sensing images. This is because: (1) Geospatial variables are highly correlated with RcNTL. For example, RcNTL itself characterizes the distance decay phenomenon of population as that modeled by the distance to city center (Fig. 2). Similarly the spatial distribution of urban land includes information provided by geophysical factors (e.g., slope) in determining population distribution (Yang et al., 2013). Therefore, some of the geospatial variables are redundant to RcNTL. (2) RcNTL can effectively characterize the localized spatial variation of population as shown in Fig. 2. However, integrating geospatial variables (e.g., distance to city center, distance to road) may eliminate these local variations. Firstly, distance to city center can only model a smoothed distance decay function but omits the local variation (for example the low value of Temple of Heaven Park). Secondly, relationships between population density and geospatial variables are spatially varied (Dong et al., 2010; Lo, 2008). For example, parameters controlling the magnitude of population decrease with the increase of distance to urban center are different in different directions of the city and in different cities, but they are estimated as the same by global statistical model.

5.2. Spatiotemporal change of urban population during 2000 and 2010 in China

Fig. 5 shows the spatial distribution of urban population at 1 km resolution in China and the three metropolitan areas in 2010. It clearly shows the regional variations with a majority of urban population residing in eastern China. The provincial capitals were hotspots of urban population and most of them had population density larger than 30,000 per km^2 in the urban centers. Locally, urban population showed strong spatial variations within the city, following the well-known distance decay phenomenon that urban population density is the highest in urban center and decreases with the increase of distance to the urban center (Fig. 5).

Urban population in China increased by 0.21 billion during the period of 2000 and 2010. This increase mainly took place in the highly urbanized regions such as Beijing-Tianjin-Tangshan, Yangtze River Delta, Pearl River Delta, and other provincial capitals (Fig. 6). This is not surprising as the highly developed areas usually have more socioeconomic opportunities and can attract more population (Hui et al., 2015; Li et al., 2015; Schneider and Mertes, 2014). Urban population change showed strong regional inequality with eastern China accounting for almost half of the increase. This posed a great challenge for the Chinese government to balance the development among regions. Urban population change also displayed strong local variations. Population in urban centers decreased significantly (Fig. 6), consistent with the observations reported in large cities using township population data in China (Wang and Zhou, 1999; Yang et al., 2013) and other countries (Lloyd et al., 2017). The major reason for this decrease is due to the governments' urban planning, which aims to decrease population density in urban center to improve urban environment. Urban population in some small towns also decreased after people moving to big cities for better socioeconomic opportunities. The decreased urban population in urban center and small towns accelerated the "pancake" style urban expansion in big cities, which is recognized as an important cause of many environmental problems (e.g., traffic congestion, air pollution, increasing commutation cost) in China.

6. Summary and conclusions

In this study we created a gridded urban population dataset with 1 km resolution for China in year 2000 and 2010, by pycnophylactically disaggregating county-level urban population using RcNTL and urban land as auxiliary datasets. The accuracy assessment using subdistrict-level population in Beijing as reference showed a mean relative error of 38% and a R^2 of 68%, demonstrating this approach can produce reasonable accuracy. The created gridded datasets avoids the underestimation of urban population by disaggregating total population especially in

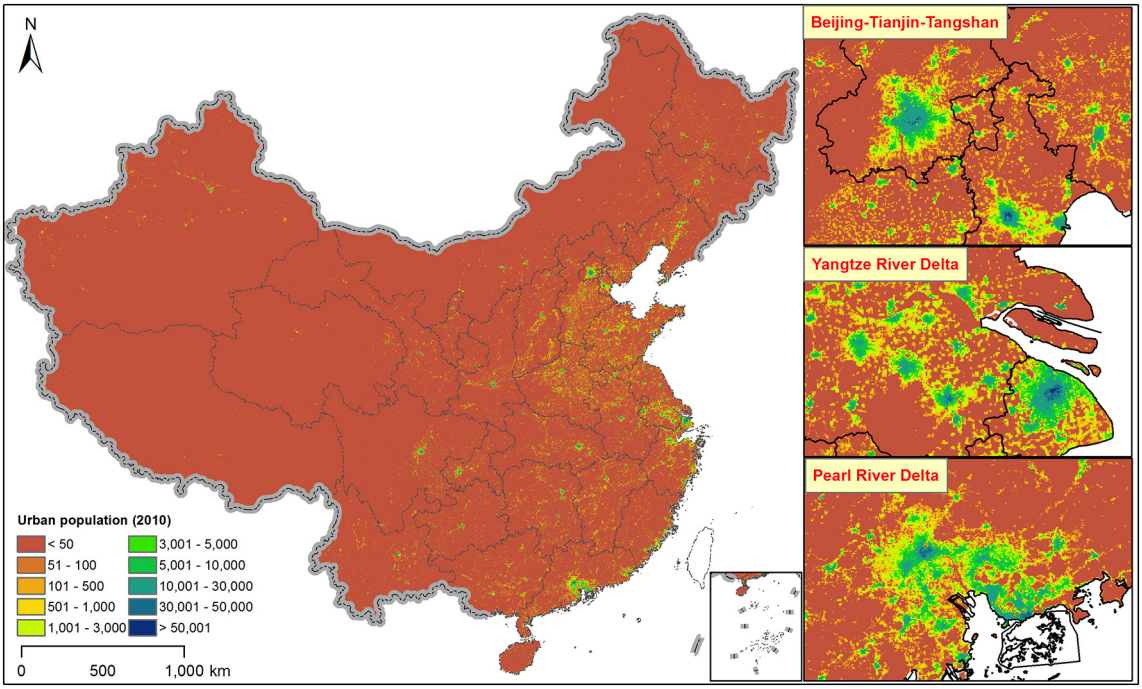

Fig. 5. Spatial distribution of the disaggregated urban population in China in 2010.

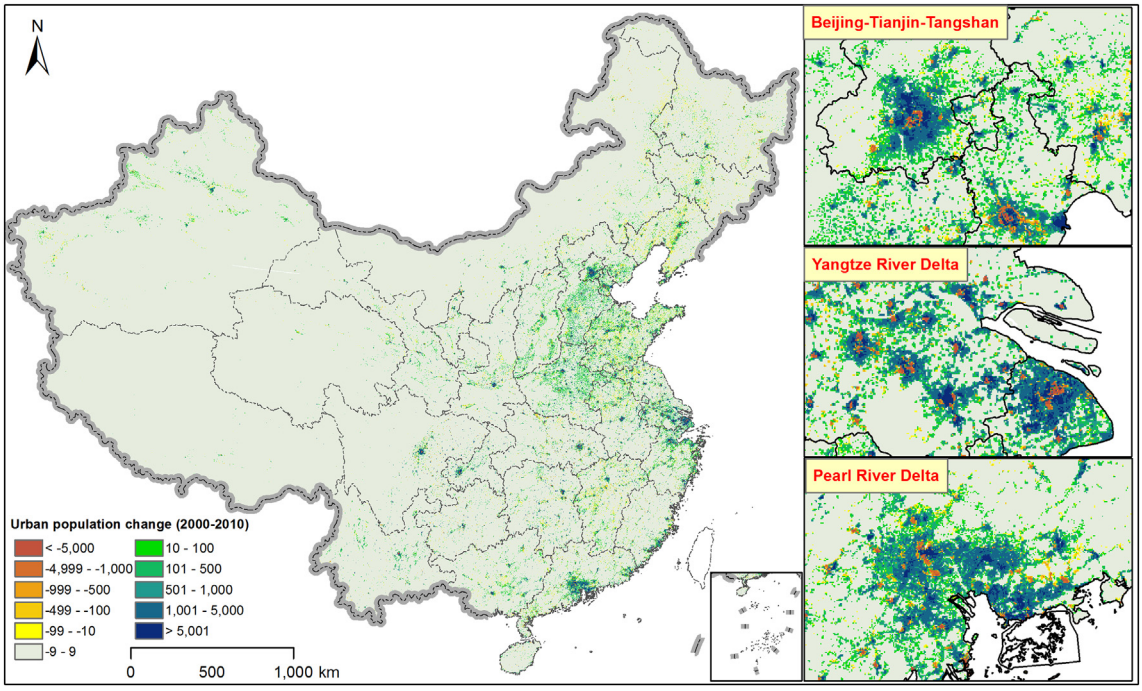

Fig. 6. Spatial distribution of urban population change in China during 2000 and 2010.

developing countries and is valuable for studying urbanization process (e.g. the national urban population change at 1 km resolution) and designing effective decision for urban planning and management.

We proposed an index of UNTL as weight to disaggregate census urban population. Comparing to the weight layer produced by statistical analysis using geospatial variables (e.g., LULC, distance to city center, slope) and remote sensing data as explanatory variables, UNTL is simple, straightforward, and less computing intensive. As the two datasets used in this study are widely accessible globally, the method has great potential to produce similar urban population dataset for other developing countries where fine scale census population datasets are scarce. It shall be noted that this approach may be not needed for developed countries where the widely available census population is reported for spatial unit with size equal to or even smaller than 1 km^2 (Mennis, 2015; Pavía and Cantarino, 2017).

It should be noted that the created urban population dataset has a spatial resolution of 1 km similar to most gridded population datasets disaggregated based on DMSP NTL and geospatial data (Sun et al., 2017; Sutton, 1997; Tan et al., 2018; Wang et al., 2018; Yu et al., 2018), because the major auxiliary data used (i.e., RcNTL in this study), has a spatial resolution of 1 km and resampling it to match the spatial resolution of the land cover data (i.e., 30 m) only slightly increased the accuracy (Fig. S2 in Supplementary data) but increased the time cost dramatically for the national application of China. The created urban population dataset measures an aggregated number of urban population for the 1 km^2 grid and has limitations in capturing the detailed spatial variation of population at building scale. However, it is still valuable, especially for large area study. For example it can be used to study the spatiotemporal pattern of urban population with reasonable details at the national scale (Wang et al., 2018; Yu et al., 2018). In addition, it can be directly integrated with other environmental datasets (e.g., temperature, air pollutant, etc.) with a similar spatial resolution to model the impact of urban environment change, for example on public health (Laaidi et al., 2012; Lin et al., 2015). However, future research on increasing the spatial resolution of the created urban population dataset is warranted. One option is using NTL data with higher spatial resolution, for example that from the Visible Infrared Imaging Radiometer Suite (VIIRS) sensor on the Suomi National Polar-orbiting Partnership (NPP) Satellite (Ma et al., 2014). The other potential option is using the increasingly available geospatial big data (e.g., point of interesting data) as weight to dasymetrically map urban population with finer spatial resolution (Bakillah et al., 2014; Yao et al., 2017).

Acknowledgment

This study is funded by the projects "Developing key technologies for establishing ecological security patterns at the Beijing-Tianjin-Hebei urban megaregion" of the National Key Research and Development Program (2016YFC0503004), the Key Research Program of Frontier Sciences, CAS (QYZDB-SSW-DQC034), the International Postdoctoral Exchange Fellowship Program (2013) of the Office of China Postdoctoral Council, and the MEP/CAS project "Survey and Assessment of National Ecosystem Changes Between 2000 and 2010, China". We would like to thank two anonymous reviewers for their constructive comments and suggestions, and the many colleagues and organizations that shared the data used in this project.

Appendix A. Supplementary data

Supplementary data to this article can be found online at https://doi.org/10.1016/j.scitotenv.2018.06.244.

References

Acuto, M., Parnell, S., Seto, K.C., 2018. Building a global urban science. Nature Sustain. 1, 2–4.

Alahmadi, M., Atkinson, P., Martin, D., 2013. Estimating the spatial distribution of the population of Riyadh, Saudi Arabia using remotely sensed built land cover and height data. Comput. Environ. Urban. Syst. 41, 167–176.

Astrudmaantay, J., Maroko, A.R., Herrmann, Christopher, 2007. Mapping population distribution in the urban environment: the cadastral-based expert dasymetric system (CEDS). Am. Cartograph. 34, 77–102.

Azar, D., Graesser, J., Engstrom, R., Comenetz, J., Leddy, R.M., Schechtman, N.G., Andrews, T., 2010. Spatial refinement of census population distribution using remotely sensed estimates of impervious surfaces in Haiti. Int. J. Remote Sens. 31, 5635–5655.

Azar, D., Engstrom, R., Graesser, J., Comenetz, J., 2013. Generation of fine-scale population layers using multi-resolution satellite imagery and geospatial data. Remote Sens. Environ. 130, 219–232.

Bajat, B., Hengl, T., Kilibarda, M., Krunić, N., 2011. Mapping population change index in Southern Serbia (1961–2027) as a function of environmental factors. Comput. Environ. Urban. Syst. 35, 35–44.
Bajat, B., Krunić, N., Samardzić-Petrović, M., Kilibarda, M., 2013. Dasymetric modelling of population dynamics in urban areas. Geodetski Vestnik 57, 777–792.
Bakillah, M., Liang, S., Mobasheri, A., Arsanjani, J.J., Zipf, A., 2014. Fine-resolution population mapping using OpenStreetMap points-of-interest. Int. J. Geogr. Inf. Sci. 28, 1940–1963.
Balk, D.L., Deichmann, U., Yetman, G., Pozzi, F., Hay, S.I., Nelson, A., 2006. Determining global population distribution: methods, applications and data. In: Hay, A.G. Simon I., David, J.R. (Eds.), Advances in Parasitology. Academic Press, pp. 119–156.
Bhaduri, B., Bright, E., Coleman, P., Urban, M., 2007. LandScan USA: a high-resolution geospatial and temporal modeling approach for population distribution and dynamics. GeoJournal 69, 103–117.
Biljecki, F., Arroyo Ohori, K., Ledoux, H., Peters, R., Stoter, J., 2016. Population estimation using a 3D city model: a multi-scale country-wide study in the Netherlands. PLoS One 11, e0156808.
Briggs, D.J., Gulliver, J., Fecht, D., Vienneau, D.M., 2007. Dasymetric modelling of small-area population distribution using land cover and light emissions data. Remote Sens. Environ. 108, 451–466.
Bright, E.A., Coleman, P.R., Rose, A.N., Urban, M.L., 2011. LandScan 2010. Oak Ridge National Laboratory, Oak Ridge, TN.
Bryan, J., Brian, C.O.N., 2013. Historically grounded spatial population projections for the continental United States. Environ. Res. Lett. 8, 044021.
Calka, B., Bielecka, E., Zdunkiewicz, K., 2016. Redistribution population data across a regular spatial grid according to buildings characteristics. Geod. Cartogr. 65.
Cao, Z., Wu, Z., Kuang, Y., Huang, N., Wang, M., 2016. Coupling an intercalibration of radiance-calibrated nighttime light images and land use/cover data for modeling and analyzing the distribution of GDP in Guangdong, China. Sustain. For. 8, 108.
CIESIN, 2017. Gridded Population of the World, Version 4 (GPWv4): Population Count, Revision 10. NASA Socioeconomic Data and Applications Center (SEDAC), Palisades, NY.
Cockx, K., Canters, F., 2015. Incorporating spatial non-stationarity to improve dasymetric mapping of population. Appl. Geogr. 63, 220–230.
Creutzig, F., Baiocchi, G., Bierkandt, R., Pichler, P.-P., Seto, K.C., 2015. Global typology of urban energy use and potentials for an urbanization mitigation wedge. Proc. Natl. Acad. Sci. 112, 6283–6288.
Deng, X., Huang, J., Rozelle, S., Zhang, J., Li, Z., 2015. Impact of urbanization on cultivated land changes in China. Land Use Policy 45, 1–7.
Dmowska, A., Stepinski, T.F., 2017. A high resolution population grid for the conterminous United States: the 2010 edition. Comput. Environ. Urban. Syst. 61, 13–23.
Dobson, J.E., Coleman, P.R., Durfee, R.C., Worley, B.A., 2000. LandScan: a global population database for estimating populations at risk. Photogramm. Eng. Remote. Sens. 66, 849–857.
Dong, P., Ramesh, S., Nepali, A., 2010. Evaluation of small-area population estimation using LiDAR, Landsat TM and parcel data. Int. J. Remote Sens. 31, 5571–5586.
Dong, N., Yang, X., Cai, H., Wang, L., 2015. A novel method for simulating urban population potential based on urban patches: a case study in Jiangsu Province, China. Sustain. For. 7, 3984.
Eicher, C.L., Brewer, C.A., 2001. Dasymetric mapping and areal interpolation: implementation and evaluation. Am. Cartograph. 28, 125–138.
Elvidge, C.D., Baugh, K.E., Dietz, J.B., Bland, T., Sutton, P.C., Kroehl, H.W., 1999. Radiance calibration of DMSP-OLS low-light imaging data of human settlements. Remote Sens. Environ. 68, 77–88.
Filip, B., Ken, A.O., Hugo, L., Ravi, P., Jantien, S., 2016. Population estimation using a 3D city model: a multi-scale country-wide study in the Netherlands. PLoS One 11, e0156808.
Gallego, F., 2010. A population density grid of the European Union. Popul. Environ. 31, 460–473.
Gallego, F.J., Batista, F., Rocha, C., Mubareka, S., 2011. Disaggregating population density of the European Union with CORINE land cover. Int. J. Geogr. Inf. Sci. 25, 2051–2069.
Gaughan, A.E., Stevens, F.R., Linard, C., Jia, P., Tatem, A.J., 2013. High resolution population distribution maps for Southeast Asia in 2010 and 2015. PLoS One 8, e55882.
Gaughan, A.E., Stevens, F.R., Huang, Z., Nieves, J.J., Sorichetta, A., Lai, S., Ye, X., Linard, C., Hornby, G.M., Hay, S.I., 2016. Spatiotemporal patterns of population in mainland China, 1990 to 2010. Sci. Data 3, 160005.
Grimm, N.B., Faeth, S.H., Golubiewski, N.E., Redman, C.L., Wu, J., Bai, X., Briggs, J.M., 2008. Global change and the ecology of cities. Science 319, 756–760.
Güneralp, B., Zhou, Y., Ürge-Vorsatz, D., Gupta, M., Yu, S., Patel, P.L., Fragkias, M., Li, X., Seto, K.C., 2017. Global scenarios of urban density and its impacts on building energy use through 2050. Proceedings of the National Academy of Sciences.
Harvey, J.T., 2002. Estimating census district populations from satellite imagery: some approaches and limitations. Int. J. Remote Sens. 23, 2071–2095.
Holt, J.B., Lo, C.P., Hodler, T.W., 2004. Dasymetric estimation of population density and areal interpolation of census data. Cartogr. Geogr. Inf. Sci. 31, 103–121.
Hsu, F.-C., Baugh, K.E., Ghosh, T., Zhizhin, M., Elvidge, C.D., 2015. DMSP-OLS radiance calibrated nighttime lights time series with intercalibration. Remote Sens. 7, 1855–1876.
Huang, Q., Yang, Y., Li, Y., Gao, B., 2016. A simulation study on the urban population of China based on nighttime light data acquired from DMSP/OLS. Sustain. For. 8, 521.
Hui, E.C., Wu, Y., Deng, L., Zheng, B., 2015. Analysis on coupling relationship of urban scale and intensive use of land in China. Cities 42, 63–69.
Joseph, M., Wang, L., Wang, F., 2012. Using Landsat imagery and census data for urban population density modeling in port-au-prince, Haiti. Mapp. Sci. Remote. Sens. 49, 228–250.
Kressler, F., Steinnocher, K., 2008. Object-Oriented Analysis of Image and LiDAR Data and its Potential for a Dasymetric Mapping Application. Springer Berlin Heidelberg.
Laaidi, K., Zeghnoun, A., Dousset, B., Bretin, P., Vandentorren, S., Giraudet, E., Beaudeau, P., 2012. The impact of Heat Islands on mortality in Paris during the August 2003 heat wave. Environ. Health Perspect. 120, 254–259.
Langford, M., 2007. Rapid facilitation of dasymetric-based population interpolation by means of raster pixel maps. Comput. Environ. Urban. Syst. 31, 19–32.
Langford, M., Higgs, G., Radcliffe, J., White, S., 2008. Urban population distribution models and service accessibility estimation. Comput. Environ. Urban. Syst. 32, 66–80.
Li, L., Lu, D., 2016. Mapping population density distribution at multiple scales in Zhejiang Province using Landsat Thematic Mapper and census data. Int. J. Remote Sens. 37, 4243–4260.
Li, H., Wei, Y.D., Liao, F.H., Huang, Z., 2015. Administrative hierarchy and urban land expansion in transitional China. Appl. Geogr. 56, 177–186.
Lin, J., Cromley, R.G., 2015. Evaluating geo-located Twitter data as a control layer for areal interpolation of population. Appl. Geogr. 58, 41–47.
Lin, C., Li, Y., Yuan, Z., Lau, A.K.H., Li, C., Fung, J.C.H., 2015. Using satellite remote sensing data to estimate the high-resolution distribution of ground-level PM2.5. Remote Sens. Environ. 156, 117–128.
Lloyd, C.D., Catney, G., Williamson, P., Bearman, N., 2017. Exploring the utility of grids for analysing long term population change. Comput. Environ. Urban. Syst. 66, 1–12.
Lo, C., 2008. Population estimation using geographically weighted regression. GI Sci. Remote. Sens. 45, 131–148.
Lu, Z., Im, J., Quackenbush, L., 2011. A volumetric approach to population estimation using LiDAR remote sensing. Photogramm. Eng. Remote. Sens. 77, 1145–1156.
Lung, T., Lübker, T., Ngochoch, J.K., Schaab, G., 2013. Human population distribution modelling at regional level using very high resolution satellite imagery. Appl. Geogr. 41, 36–45.
Ma, T., Zhou, C., Pei, T., Haynie, S., Fan, J., 2014. Responses of Suomi-NPP VIIRS-derived nighttime lights to socioeconomic activity in China's cities. IEEE Geosci. Remote Sens. Lett. 5, 165–174.
Maantay, J., Maroko, A., 2009. Mapping urban risk: flood hazards, race, & environmental justice in New York. Appl. Geogr. 29, 111.
Mao, Y., Ye, A., Xu, J., 2012. Using land use data to estimate the population distribution of China in 2000. GI Sci. Remote. Sens. 49, 822–853.
McKee, J.J., Rose, A.N., Bright, E.A., Huynh, T., Bhaduri, B.L., 2015. Locally adaptive, spatially explicit projection of US population for 2030 and 2050. Proc. Natl. Acad. Sci. 112, 1344–1349.
Mennis, J., 2009. Dasymetric mapping for estimating population in small areas. Geograph. Compass 3, 727–745.
Mennis, J., 2010. Generating surface models of population using dasymetric mapping. Prof. Geogr. 55, 31–42.
Mennis, J., 2015. Increasing the accuracy of urban population analysis with dasymetric mapping. City 17.
Mennis, J., Hultgren, T., 2006. 'Intelligent' dasymetric mapping and its comparison to other areal interpolation techniques. Proceedings of Autocarto.
Nagle, N.N., Buttenfield, B.P., Leyk, S., Spielman, S., 2014. Dasymetric modeling and uncertainty. Ann. Assoc. Am. Geogr. 104, 80–95.
NBSC, 2002. Tabulation on the 2000 Population Census of the People's Republic of China. China Statistics Press, Beijing.
NBSC, 2012. Tabulation on the 2010 Population Census of the People's Republic of China. China Statistics Press, Beijing.
Ouyang, Z., Zheng, H., Xiao, Y., Polasky, S., Liu, J., Xu, W., Wang, Q., Zhang, L., Xiao, Y., Rao, E., Jiang, L., Lu, F., Wang, X., Yang, G., Gong, S., Wu, B., Zeng, Y., Yang, W., Daily, G.C., 2016. Improvements in ecosystem services from investments in natural capital. Science 352, 1455–1459.
Pavía, J.M., Cantarino, I., 2017. Can dasymetric mapping significantly improve population data reallocation in a dense urban area? Geogr. Anal. 49, 155–174.
Qi, W., Liu, S., Gao, X., Zhao, M., 2015. Modeling the spatial distribution of urban population during the daytime and at night based on land use: a case study in Beijing, China. J. Geogr. Sci. 25, 756–768.
Reibel, M., Bufalino, M.E., 2005. Street-weighted interpolation techniques for demographic count estimation in incompatible zone systems. Environ. Plan. A 37, 127–139.
Ruther, M., Leyk, S., Buttenfield, B.P., 2015. Comparing the effects of an NLCD-derived dasymetric refinement on estimation accuracies for multiple areal interpolation methods. Mapp. Sci. Remote. Sens. 52, 158–178.
Salvatore, M., Pozzi, F., Ataman, E., Huddleston, B., Bloise, M., Balk, D., Brickman, M., Anderson, B., Yetman, G., 2005. Mapping Global Urban and Rural Population Distributions. FAO, Rome.
Schneider, A., Mertes, C.M., 2014. Expansion and growth in Chinese cities, 1978–2010. Environ. Res. Lett. 9, 024008.
Schroeder, J.P., 2007. Target-density weighting interpolation and uncertainty evaluation for temporal analysis of census data. Geogr. Anal. 39, 311–335.
Seto, K.C., Dhakal, S., Bigio, A., Blanco, H., Delgado, G.C., Dewar, D., Huang, L., Inaba, A., Kansal, A., Lwasa, S., 2014. Human settlements, infrastructure and spatial planning. In: Edenhofer, O., et al. (Eds.), Climate Change 2014: Mitigation of Climate Change, Contribution of Working Group III to the Fifth Assessment Report of the Intergovernmental Panel on Climate Change.
Silva, F.B.e., Gallego, J., Lavalle, C., 2013. A high-resolution population grid map for Europe. J. Maps 9, 16–28.
Song, G., Yu, M., Liu, S., Zhang, S., 2015. A dynamic model for population mapping: a methodology integrating a Monte Carlo simulation with vegetation-adjusted nighttime light images. Int. J. Remote Sens. 36, 4054–4068.
Stevens, F.R., Gaughan, A.E., Linard, C., Tatem, A.J., 2014. Disaggregating census data for population mapping using random forests with remotely-sensed and ancillary data. PLoS One 10, e0107042.

Stevens, F., Gaughan, A., Linard, C., Tatem, A., 2015. Disaggregating census data for population mapping using random forests with remotely-sensed and ancillary data. PLoS One 10, e0107042.
Su, M.-D., Lin, M.-C., Hsieh, H.-I., Tsai, B.-W., Lin, C.-H., 2010. Multi-layer multi-class dasymetric mapping to estimate population distribution. Sci. Total Environ. 408, 4807–4816.
Sun, W., Zhang, X., Wang, N., Cen, Y., 2017. Estimating population density using DMSP-OLS night-time imagery and land cover data. IEEE J. Sel. Top. Appl. Earth Observ. Remote. Sens. 10 (6), 2674–2684.
Sutton, P., 1997. Modeling population density with night-time satellite imagery and GIS. Comput. Environ. Urban. Syst. 21, 227–244.
Sutton, P., Roberts, D., Elvidge, C., Melj, H., 1997. A comparison of nighttime satellite imagery and population density for the continental United States. Photogramm. Eng. Remote. Sens. 63, 1303–1313.
Tan, M., Li, X., Li, S., Xin, L., Wang, X., Li, Q., Li, W., Li, Y., Xiang, W., 2018. Modeling population density based on nighttime light images and land use data in China. Appl. Geogr. 90, 239–247.
Tatem, A.J., Noor, A.M., Von Hagen, C., Di Gregorio, A., Hay, S.I., 2007. High resolution population maps for low income nations: combining land cover and census in East Africa. PLoS One 2, e1298.
Tomás, L., Fonseca, L., Almeida, C., Leonardi, F., Pereira, M., 2016. Urban population estimation based on residential buildings volume using IKONOS-2 images and lidar data. Int. J. Remote Sens. 37, 1–28.
United Nations, 2014. World Urbanization Prospects: The 2014 Revision. Population Division of the Department of Economic and Social Affairs of the United Nations Secretariat.
Ural, S., Hussain, E., Shan, J., 2011. Building population mapping with aerial imagery and GIS data. Int. J. Appl. Earth Obs. Geoinf. 13, 841–852.
Wang, F., Zhou, Y., 1999. Modelling urban population densities in Beijing 1982–90: suburbanisation and its causes. Urban Stud. 36, 271–287.
Wang, L., Wang, S., Zhou, Y., Liu, W., Hou, Y., Zhu, J., Wang, F., 2018. Mapping population density in China between 1990 and 2010 using remote sensing. Remote Sens. Environ. 210, 269–281.
Wright, J.K., 1936. A method of mapping densities of population with cape cod as an example. Geogr. Rev. 26, 103–110.
Wu, S.-s., Qiu, X., Wang, L., 2005. Population estimation methods in GIS and remote sensing: a review. GI Sci. Remote. Sens. 42, 80–96.
Wu, B., Yuan, Q., Yan, C., Wang, Z., Yu, X., Li, A., Ma, R., Huang, J., Chen, J., Chang, C., Liu, C., Zhang, L., Li, X., Zeng, Y., Bao, A., 2014. Land cover changes of China from 2000 to 2010. J. Quat. Sci. 34, 723–731 (In Chinese with English abstract).
Xu, W., Xiao, Y., Zhang, J., Yang, W., Zhang, L., Hull, V., Wang, Z., Zheng, H., Liu, J., Polasky, S., Jiang, L., Xiao, Y., Shi, X., Rao, E., Lu, F., Wang, X., Daily, G.C., Ouyang, Z., 2017. Strengthening protected areas for biodiversity and ecosystem services in China. Proc. Natl. Acad. Sci. 114, 1601–1606.
Yang, X., Yue, W., Gao, D., 2013. Spatial improvement of human population distribution based on multi-sensor remote-sensing data: an input for exposure assessment. Int. J. Remote Sens. 34, 5569–5583.
Yao, Y., Liu, X., Li, X., Zhang, J., Liang, Z., Mai, K., Zhang, Y., 2017. Mapping fine-scale population distributions at the building level by integrating multisource geospatial big data. Int. J. Geogr. Inf. Sci. 31, 1220–1244.
Yu, S., Zhang, Z., Liu, F., 2018. Monitoring population evolution in China using time-series DMSP/OLS nightlight imagery. Remote Sens. 10, 194.
Yue, T.X., Wang, Y.A., Liu, J.Y., Chen, S.P., Qiu, D.S., Deng, X.Z., Liu, M.L., Tian, Y.Z., Su, B.P., 2005. Surface modelling of human population distribution in China. Ecol. Model. 181, 461–478.
Yue, W., Liu, Y., Fan, P., 2013. Measuring urban sprawl and its drivers in large Chinese cities: the case of Hangzhou. Land Use Policy 31, 358–370.
Zandbergen, P.A., 2011. Dasymetric mapping using high resolution address point datasets. Trans. GIS *15*, 5–27.
Zeng, C., Zhou, Y., Wang, S., Yan, F., Zhao, Q., 2011. Population spatialization in China based on night-time imagery and land use data. Int. J. Remote Sens. 32, 9599–9620.
Zhuo, L., Ichinose, T., Zheng, J., Chen, J., Shi, P.J., Li, X., 2009. Modelling the population density of China at the pixel level based on DMSP/OLS non-radiance-calibrated night-time light images. Int. J. Remote Sens. 30, 1003–1018.
Zoraghein, H., Leyk, S., Ruther, M., Buttenfield, B.P., 2016. Exploiting temporal information in parcel data to refine small area population estimates. Comput. Environ. Urban. Syst. 58, 19–28.